Published in final edited form as:
Behav Neurosci. 2010 December ; 124(6): 839–850. doi:10.1037/a0021556.

Impacts of forebrain neuronal glycine transporter 1 disruption in the senescent brain: Evidence for age-dependent phenotypes in Pavlovian learning

Sylvain Dubroqua[1], **Philipp Singer**[1], **Detlev Boison**[2], **Joram Feldon**[1], **Hanns Möhler**[3,4], and **Benjamin K. Yee**[1]

[1]Laboratory of Behavioral Neurobiology, Swiss Federal Institute of Technology Zurich, Schorenstrasse 16, 8603 Schwerzenbach, Switzerland [2]R.S. Dow Neurobiology Laboratories, Legacy Research, 1225 NE 2nd Avenue, Portland, OR 97232, United States [3]Institute of Pharmacology and Toxicology, University of Zurich, Winterthurerstrasse 190, 8057 Zurich, Switzerland [4]Institute of Pharmaceutical Sciences, Collegium Helveticum ETH Zurich, Semper-Sternwarte, Schmelzbergstrasse 25, CH-8092 Zurich, Switzerland

Abstract

Genetic deletion of glycine transporter 1 (GlyT1) in forebrain neurons gives rise to multiple pro-cognitive phenotypes, presumably due to enhanced *N*-methyl-D-aspartate receptor (NMDAR) functions. However, concerns over possible harmful excitotoxic effects under life-long elevation of synaptic glycine have been raised. Such effects might accelerate the aging process, weakening or even reversing the pro-cognitive phenotypes identified in adulthood. Here, we examined if one of the most robust phenotypes in the mutant mouse line (CamKIIαCre;GlyT1tm1.2fl/fl), namely, enhanced aversive Pavlovian conditioning, might be modified by age. Comparison between 3-month-old (adult) and 22-month-old (aged) mutants confirmed the presence of this phenotype at both ages. However, the temporal expression of the Pavlovian phenotype was modified in senescence; while adult mutants showed a pronounced within-session extinction, aged mutants did not. Expression of NR2B subunits of NMDAR and neural proliferation were examined in the same animals by immunohistochemistry. These were reduced in the aged mice as expected, but not exacerbated by the mutation. Thus, our results do not substantiate the concerns of neurotoxic effects through life-long GlyT1 disruption in forebrain neurons, but provide evidence for a modification of phenotypic expression as a function of age. The latter points raise the need to further investigate other pro-cognitive phenotypes identified at adulthood in this mutant line. In addition, we revealed here for the first time a clear increase in the number of immature neurons in the hippocampus of the mutants, although the behavioral significance of this phenotype remains to be determined.

Keywords

Cognitive enhancement; Glycine; Learning; NMDA receptor; Senescence

Correspondence to BKY at: Laboratory of Behavioral Neurobiology ETH Zurich, Schorenstrasse 16, 8603 Schwerzenbach, Switzerland, byee@ethz.ch, ☎: +41 44 655 74 17, fax: +41 44 655 73 02.

Introduction

N-methyl-D-aspartate receptor (NMDAR) -dependent synaptic plasticity has been implicated in various forms of learning and memory processes (Morris, 1989; Morris, Anderson, Lynch, & Baudry, 1986). Its hypofunction may be associated with the cognitive deficiency characteristic of a number of psychiatric disorders, such as schizophrenia, as well as with the course of normal aging (Rosenzweig & Barnes, 2003). Enhancing NMDAR function therefore represents a possible strategy to ameliorate such deficits (Martin, Grimwood, & Morris, 2000). While direct activation of NMDARs is prone to severe side effects including neurotoxicity and seizures (Rothman & Olney, 1995), modulation of NMDAR function via allosteric sites offers an opportunity for alternative pharmacological targets (Yang & Svensson, 2008). One strategy is to increase the availability of glycine in the vicinity of NMDARs, and therefore the occupancy of the co-agonist glycine-B site of the NMDAR complex. This can be effectively achieved by pharmacological inhibition of glycine re-uptake via glycine transporter 1 (GlyT1) which co-localizes with NMDARs in neurons. Such inhibition has been reported to enhance NMDAR excitability, confer resistance to behavioral deficits induced by NMDAR antagonists, and lead to some forms of enhanced cognitive performance (Black *et al.*, 2009; Depoortere *et al.*, 2005; Singer, Boison, Mohler, Feldon, & Yee, 2009).

We have recently shown that disruption of GlyT1 restricted to forebrain neurons is sufficient to facilitate performance on various cognitive processes, including Pavlovian conditioning, reversal learning, latent inhibition and memory for object identity as well as object location (Singer, Boison, Mohler, Feldon, & Yee, 2007; Singer *et al.*, 2009; Yee *et al.*, 2006). When GlyT1 is knocked out in the entire forebrain, working memory function is also enhanced (Singer *et al.*, 2009), extending an earlier report of improved reference memory retention in constitutive heterozygous GlyT1 knockout mice (Tsai *et al.*, 2004). Although direct demonstration of GlyT1 deletion or blockade alone being sufficient to induce excitotoxicity is lacking, Sanderson and Bannerman (2007) have raised concern over possible negative impacts of this manipulation in the long term. The deletion of the GlyT1 gene, in spite of its potential cognitive gain, may carry a putative ‘cost’. More specifically, GlyT1 deletion may carry a greater risk of neurodegeneration or excitotoxicity, especially in aged animals, outweighing any potential cognitive gain from enhanced NMDAR activation (Javitt, 2004). Increasing Ca^{2+} influx through NMDARs and perhaps AMPA receptors may lead to excitotoxicity and neuronal death implicated in neurodegenerative disorders such as Alzheimer's disease (Javitt, 2004). A life-long elevation of glycine concentration in the vicinity of NMDARs might be apoptotic. This hypothesis is highly relevant to the potential clinical application of GlyT1-inhibitors as cognitive enhancers or antipsychotic drugs. The present study is designed to address empirically two critical implications raised by Sanderson and Bannerman (2007).

In the present study we first examined if the cognitive enhancing effects of GlyT1 disruption demonstrated in adult animals might be modified in senescence, as would be expected if the genetic disruption did carry long-term negative impact. A diminution, absence or even reversal of such an effect in aged subjects would lend some credence to Sanderson and Bannerman's (2007) concern. To this end, we compared the behavioral effects seen in mutant mice with forebrain neuronal GlyT1 knockout to those observed in control mice at two ages: 3 months (“adult”) vs. 22 months old (“aged”). We focused on one of the most robust pro-cognitive traits of this conditional genetic knockout, namely enhanced associative learning as exemplified by Pavlovian conditioned freezing (Yee *et al.*, 2006). Prior to the conditioning experiment, possible relevant confounding effects that might interfere with the freezing response were assessed by the elevated-plus maze test of anxiety and the open field test of spontaneous locomotors activity.

Following behavioral assessments, selected anatomical markers were assessed to gauge the putative negative impacts of long-term GlyT1 disruption in the brain. First, apoptosis related to neurotoxicity or accelerated neurodegeneration in the hippocampus was evaluated by activated caspase-3 immunohistochemistry (Budihardjo, Oliver, Lutter, Luo, & Wang, 1999). Second, density of the immuno-signals against the NR1 and NR2B subunits of the NMDAR in amygdala and prefrontal cortices in addition to hippocampus was measured. NMDARs are pertinent to the normal functioning of these brain regions, which are implicated in the acquisition and extinction of fear conditioning (Maren, 2001). Given that binding to glycine-B site primes the internalization and degradation of NMDARs (Nong *et al.*, 2003), persistent and excessive glycine-B site activation might reduce NMDAR expression. Finally, the immature neuronal marker doublecortin (DCX) was used to index neural proliferation in the dentate gyrus, which is known to be regulated by NMDAR activity, and down-regulated in senescence (Bizon & Gallagher, 2003).

Methods

Subjects

The subjects were offspring obtained by crossing CamKIIαCre:Glyt1tm1.2fl/fl mice with Glyt1tm1.2fl/fl mice (both maintained on a pure C57BL/6J background). This breeding strategy yielded litters with a 1:1 mixture of CamKIIαCre:Glyt1tm1.2fl/fl (hereafter simply referred to as “mutant”) and Glyt1tm1.2fl/fl (“control”) mice. Breeding took place in a specific-pathogen free (SPF) breeding facility (Laboratory of Behavioral Neurobiology, ETH Zurich, Schwerzenbach, Switzerland). Litters were weaned at postnatal day 21. Genotypes were determined by standard PCR on tail biopsies obtained within 10 days after weaning on postnatal day 21 as previously described (Yee *et al.*, 2006). At the age of 11 weeks, the animals were transferred to a separate climatized animal vivarium (21±1°C, relative humidity at 55±5%) under a reversed light-dark cycle (lights off: 0800–2000). They were kept in groups of 3–5 in Makrolon® Type-III cages (Techniplast, Milan, Italy), and maintained under constant ad libitum water and food (Kliba 3430, Klibamuhlen, Kaiseraugst, Switzerland). The ‘adult’ mice were approximately three-months old at the time of testing, comprising 5 male and 6 female mutant mice, and 4 male and 5 female littermate controls. The ‘aged’ mice were approximately 22-24 months of age at the time of testing, and comprised 5 male and 4 female mutant mice, and 7 male and 6 female littermate controls. Animals from both age groups were tested together in a single experiment. All tests were conducted in the dark phase of the light-dark cycle. The experimental manipulations and procedures described here had been previously approved by the Swiss Cantonal Veterinary Office, in accordance to the ethical standards required by the Swiss Act and Ordinance on Animal Protection and the European Council Directive 86/609/EEC, which are in accordance with the NIH Guide for the Care and Use of Laboratory Animals (1996).

The animals were subjected to the three behavioral tests as described below in the order of their implementation.

Elevated plus maze test of anxiety

General anxiety can be affected by senescence and can therefore be a potential confounding factor in the assessment of learned fear. In order to evaluate this, the elevated plus maze test was used as an ethologically relevant test of anxiety, induced by exposed spaces and height. The apparatus has been fully described elsewhere (Yee *et al.*, 2004). Briefly, it consisted of a set of four equally spaced arms (30cm long and 5 cm wide) joined to a central square platform (5 cm × 5 cm); two opposing arms were exposed and unprotected whilst the other two arms were protected by opaque side walls and an end wall at the distal end of the arm. The test began when the animal was released into the central area of the maze with its head

facing an open arm, and allowed to explore freely for 5 min before being removed and returned to the home cage. A digital camera mounted above the maze captured and transmitted images at a rate of 5Hz to a PC running the Ethovision tracking system (Noldus Technology Wageningen, The Netherlands). This allowed the computation of two standard anxiety-related measures: (i) *percent time spent in the open arms* = time in open arms / time in all four arms × 100%, and (ii) *percent number of entries into open arms* = number of open arm entries / number of all arm entries × 100%. In addition, locomotor activity was indexed by the total distance travelled on the entire maze surface during the test period. A rest period of 48 h was allowed before the assessment of the next test.

Open field test of spontaneous locomotor activity

Spontaneous activity can also be altered with senescence and become another potential confound in the measurement of immobility in the subsequent conditioned freezing experiment. This was assessed next in an open field. Four identical 40 × 40cm^2 white open field arenas with 35cm high sidewalls and a water-proof inlay were used. The animals were tested in squads of four, under diffused dim lighting at 30 lux. Allocation to the four test arenas was counterbalanced. Each mouse was gently placed in the centre of the appropriate open field and allowed to explore undisturbed for 1 h. The open fields were cleansed with water and dried after each animal. Locomotor activity was indexed by spatial displacement tracked by the EthoVision® tracking system (Version 3.1, Noldus Technology, Wageningen, The Netherlands), expressed as distance travelled (in m) across successive 10-min bins. The conditioned freezing was assessed 4 days after the open field test.

Conditioned freezing paradigm

The apparatus comprised two distinct sets of test chambers (4 per set), as fully described elsewhere (Meyer, Feldon, Schedlowski, & Yee, 2005). All chambers were equipped with a grid floor composed of stainless steel rods spaced at 10-mm intervals, and through which scrambled electric shocks (unconditioned stimulus, US) could be delivered (Model E13-14, Coulbourn Instruments). C57BL/6 mice are known however to suffer from a progressive deterioration in hearing that begins at about 2 months of age and significant hearing impairment is expected by the age of 18 months (Walton, Barsz, & Wilson, 2008). A clear hearing loss in the aged mutant and control mice was confirmed by the presence of a pronounced deficit in the acoustic startle response in comparison to the adult mice (data not shown). Hence, the use of an auditory conditioned stimulus would have been inappropriate in this test, and instead a tactile stimulus in the form of a high-frequency vibration of the grid floor was used as the conditioned stimulus (CS). This was achieved by fixing a commercial vibrating unit (MiniVibrator Model 558095, Orion Versand AG, Buchs, Switzerland) to the grid floor (Yee, Singer, Chen, Feldon, & Boison, 2007). Transmission of the sinusoidal vibration beyond the grid floor was dampened by insulating the grid from the test chamber floor on four pieces of shock-absorbing sponge. A constant background white noise (60 dB) was provided via a loudspeaker mounted inside each chamber to mask the weak noise emitted from the vibrating unit. A digital camera was mounted 30 cm directly above the area of interest in each chamber. Digital images were captured at a rate of 1 Hz and transmitted to a PC running the Windows XP (SP3) operating system via a Picolo™ frame grabber (Euresys s.a., Liège, Belgium). An image analysis algorithm originally described by Richmond et al (1998) was used to determine freezing (immobility) in real-time. The image analysis was performed using Open eVision 1.1 (Euresys s.a., Liège, Belgium) under the control of a customized Microsoft Visual Basic (version 6) script.

On day 1, the animals received two discrete trials of CS-US pairing. Each trial comprised a 30-s CS followed immediately by a 1-s foot-shock set at 0.25mA. Each trial was preceded and followed by a 180s interval. On day 2, the animals were returned to the same chambers

and observed for a period 480s in the absence of any discrete stimulus to assess conditioned freezing to the training context. On day 3, the animals were placed in a novel and distinct conditioning chamber to measure the conditioned freezing response specific to the CS. Following an initial 120-s acclimatization period, the CS was presented continuously for 480s. Freezing behavior during the pre-CS and CS periods were separately evaluated. A second CS test was repeated 24h later (i.e., on day 4). After successful demonstration of the retention of extinction from the first to the second CS tests (i.e., between-days extinction), we went on to examine spontaneous recovery (re-emergence of an extinguished CR) by conducting a third CS test, 7 days later. Given evidence for an extinction phenotype in our mutant mice, the test of spontaneous recovery allowed the examination of the dissipation of the inhibitory mechanism implicated in extinction learning.

Neuroanatomy

Due to advanced age 3 animals (1 female control and 2 male mutant aged mice) died in the week following completion of behavioral testing. The remaining animals were deeply anesthetized with sodium pentobarbital (Nembutal®; 40 mg/kg, i.p.) and then perfused transcardially: first with 0.9% NaCl saline, followed by a cold 0.15M phosphate buffered (pH 7.4) fixative solution containing 4% paraformaldehyde and 15% saturated picric acid solution. Perfusion of one animal (an adult female mutant) was not satisfactory and as a result the brain was not further processed. The brains extracted from 19 adult mice (control male n=4, control female n=5, mutant male n=5, mutant female n=5) and 19 aged mice (control male n=7, control female n=5, mutant male n=3, mutant female n=4) were post-fixed for 24h before being subjected to microwave-assisted fixation as previously described (Fritschy, Weinmann, Wenzel, & Benke, 1998). The brains were then immersed in 30% sucrose solution for cryoprotection until sectioning. Eight series of free-floating 30μm thick coronal sections, spanning approximately from 2.22mm to 7.08mm anterior to bregma, were cut using a freezing microtome. The sections were then kept at -20°C until immunohistochemical processing.

Immunohistochemistry for each marker was performed on one series of sections per animal. The following primary antibodies were used: goat anti-doublecortin (DCX) (1:1000; Santa Cruz Biotechnology, Santa Cruz, USA), rabbit anti-cleaved Caspase-3 (1:600; Cell Signaling Technology, Beverly, MA), rabbit anti-NMDA Receptor subunit type 1 (NR1) (1:4000; ABR, USA), rabbit anti-NMDA Receptor subunit type 2B (NR2B) (1:1000; ABR, USA). Sections destined for NR1 and NR2B immunostaining were first rinsed in Tris buffer for 10 min × 3, whereas sections destined for Caspase-3 and DCX immunostaining were similarly washed in phosphate buffered saline. Endogenous peroxidases were blocked via incubation in a phosphate buffer containing 10% (v/v) of 33% H_2O_2 for 10 min. Next, the sections were incubated in 0.3% Triton X-100 containing 10% normal serum for 1h at room temperature (RT). The appropriate primary antibodies were then diluted in a buffer containing 0.3% Triton X-100 and 2% normal serum. The sections were incubated overnight at RT (DCX, caspase3) or 4°C (NR1 and NR2B). After three washes in buffer solution (10 min each), the sections were incubated for 1h with the biotinylated secondary antibody diluted 1:500 in a buffer containing 2% normal serum and 0.3% Triton X-100. Sections were washed three times for 10 min, and then incubated with the Vectastain kit (Vector Laboratories, Burligame, CA) diluted in the same buffer for 1h. After three rinses in 0.1M Tris-HCl buffer (pH 7.4), the sections were stained with 1.25% 3,3-diaminobenzidine (DAB, Fluka, Buchs, Switzerland) and 0.08% H_2O_2 in 0.1 M Tris-HCl (pH 7.6), for 2–15 min. The DAB reaction was terminated by three washes in Tris-HCl. The sections were then mounted onto gelatine-coated slides, air dried overnight, dehydrated and coverslipped with Eukitt™ (Kindler GmbH & Co, Freiburg, Germany).

All subsequent quantifications were performed blind to the genotype and age of the animals.

Stereological quantification of DCX-ir and Caspase 3-ir cells

Immunoreactive (ir) cells, identified by the presence of DAB staining in the cell nucleus, were counted in one randomly chosen hemisphere using the optical fractionator method (Gundersen *et al.*, 1988). Every section within a randomly chosen 1:8 series was counted, allowing an average of five sections per animal spanning approximately from 1.22 to 2.30 mm posterior to bregma encompassing the dorsal hippocampus. Sampling was performed with a fixed counting frame with a width of 30 μm and a length of 30 μm; and a sampling grid size of 200 × 200 μm^2 in the x-y plane. Counting was performed using a 40× oil lens (N.A. 1.30). Delineation of the region of interest (ROI) was performed under live microscopy (Zeiss Axioplan microscope) with a 2.5× objective (N.A. 0.075). Volume estimates were performed with the assistance of StereoInvestigator (version 6.50.1, Microbrightfield, Colchester, VT, USA), and application of the Cavalieri method with the formula $V = (\Sigma A \times t_{nom}) / ssf$, where ΣA = the summed areas of ROIs across sections (computed by StereoInvestigator), t_{nom} = the nominal section thickness of 30 μm, and ssf = the section sampling fraction (1/8). The ROI for the quantification of doublecortin-ir cells was restricted to the subgranular zone (SGZ) of the dentate gyrus, whereas the ROI for caspase-3-ir cells included both dentate gyrus and Ammon's horn (subfields CA1/2 and CA3). All counts were expressed in units of cell per mm^3.

Densitometry

Four to six coronal sections, extending across the prefrontal cortex, amygdala or the dorsal hippocampus, per animal were analyzed using a Zeiss Axioplan microscope equipped with a 2.5× objective. Digital images of NR1 or NR2B immuno-stained sections were acquired (Axiocam Zeiss, Germany), with the exposure times held constant during acquisition such that pixel brightness was never saturated. Densitometry measurement was then obtained in one randomly selected hemisphere by ImageJ software (National Institutes of Health, Bethesda, MD, USA). For the amygdala, pixel brightness in the basolateral nucleus (BLA) and the central nucleus (CeA) was separately measured. For the prefrontal cortex, cingulate cortex (Cg1), the prelimbic cortex (PrL) and the infralimbic cortex (IL) were separately analyzed. For the dorsal hippocampus, pixel brightness was measured in CA1/2 stratum radiatum and CA3 stratum lucidum (see Figure 5). In each case, two to three non-overlapping 100 × 100 μm^2 square grids were placed randomly in the area of interest, and the background-corrected optical densities (pixel brightness in the region of interest minus pixel brightness of the background) were computed and averaged.

Statistical analysis

All data were analyzed by parametric analysis of variance (ANOVA) using the between-subject factors genotype and age. Initial preliminary analyses also included the between-subject factor sex, but there was no evidence for any interaction effect involving sex. This factor was therefore dropped in the final analysis to increase statistical power. Additional within-subjects factors were included as appropriated by the dependent variables in question. Supplementary restricted analyses were also conducted to assist interpretation of statistically significant effects. All statistical analyses were carried out using SPSS for Windows (version 13, SPSS Inc. Chicago IL, USA) implemented on a PC running the Windows XP (SP3) operating system. Because the doublecortin data set deviated substantially from the homoscedasticity assumption of parametric ANOVA, a non-parametric ANOVA was performed on the rank-transformed data (Conover & Iman, 1981).

Results

Anxiety and spontaneous activity

Anxiety-like behavior in the elevated plus maze was indexed by the animals' reluctance to venture into the open arms relative to the enclosed arms. This was expressed by the percent time spent in the open arms, or the proportion of arms entries into the open arms (Table 1). Separate 2 × 2 (age × genotype) ANOVAs of the two measures did not yield any significant effect [F's<1]. Thus, neither genotype nor age significantly modified the expression of anxiety. Similarly, separate analysis of the total distance travelled in the maze was analysed, which also did not yield any significant effects [F's<1] (see Table 1), thus confirming that the test was not confounded by possible group differences in spontaneous locomotor activity.

Locomotor activity was further evaluated in the open field for a longer period of time sufficient for the assessment of locomotor habituation effect. Habituation was evident from the monotonic reduction of activity over the course of the 60 min period – an effect that was equivalently seen in all groups (see Figure 1). The overall level of activity was highly comparable across genotype as well as age groups. A 2 × 2 × 6 (age × genotype × 10-min bins) ANOVA of distance travelled only yielded a significant effect of bins [$F(5,190)=101.3$, $p<0.001$].

Potential difference in general anxiety or baseline locomotor activity might confound the measure of conditioned fear in the form of freezing in the subsequent conditioned freezing experiment. These were excluded by these two separate tests.

Conditioned freezing

Here, we focused on the conditioned freezing paradigm since this test revealed the most robust promnesic effect in adult mutants (Yee *et al.*, 2006). On the day of conditioning, the level of freezing generally increased over successive periods of inter-trial intervals (ITIs, Figures 2A). A similar increase from the first to the second CS presentation in each CU-US pairing was observed in the adult but not the aged mice (Figure 2A). Separate split-plot ANOVAs of freezing recorded during ITIs and during CS presentations yielded only a main effect of ITI periods [$F(2,76)=55.07$, $p<0.001$].

Conditioned freezing to the context was tested 24h later, and the levels of freezing obtained did not reveal any effect of genotype [$F(1,38)=1.78$, $p=0.20$]. However, there was an increase in freezing level over the course of the 8-min test that was apparent only in the adult but not aged mice (Figure 2B). A 2 × 2 × 2 (genotype × age × half-session) ANOVA of percent freezing revealed a significant age by half-session interaction [$F(1,38)=4.39$, $p<0.05$].

Next, conditioned freezing to the CS was assessed in two extinction tests conducted across consecutive days in a neutral context. Each test began with a 2-min pre-CS period allowing the evaluation of baseline freezing levels. Analysis of Pre-CS freezing by a 2 × 2 × 2 (age × genotype × days) ANOVA did not reveal any clear significant difference between the two ages [$F(1,38)=1.66$, $p=0.20$] or genotypes [$F(1,38)=4.07$, $p=0.05$]. Next, the tactile CS was presented for 8 min. The overall freezing response to the CS was stronger in the mutant mice compared with the moderate freezing levels seen in the controls (Figures 3G, 3J). However, the time course of the freezing response to the CS markedly differed between adult and aged mutant subjects (Figure 3A). Adult mutants reacted to the initiation of the CS with a pronounced freezing response which then quickly subsided in the course of the 8 min test period as a result of within-session extinction (Figure 3A) – a profile that was similarly seen on both test days. In contrast, the temporal profile of the aged mutants' freezing response

remained relatively stable over time (Figure 3A) – suggesting weaker extinction within a test session compared with adult mutants. The contrasting profile is more readily discernable in Figure 3B, which shows the within-session profile averaged across the two consecutive test days. While within-session extinction appeared weak in aged mutants, between-day extinction was still evident in all groups.

A 2 × 2 × 2 × 4 (genotype × age × days × 2-min bins) ANOVA of percent freezing revealed a significant effect of genotype [$F(1,38)=7.06$, $p<0.05$], supporting the overall presence of enhanced conditioned freezing to the CS in the mutants regardless of age. Additionally, the presence of a significant bins [$F(3,114)=7.00$, $p<0.001$] and days effects [$F(1,38)=21.35$, $p<0.001$] reflected the overall presence of both within- and between-day extinction, respectively. Lastly, evidence for age-dependent phenotypes was revealed when within-session freezing over bins was examined, as supported by the presence of a significant genotype × age × bins interaction [$F(3,114)=3.85$, $p<0.05$] (Figure 3H and 3K). Orthogonal contrast analysis indicated that this interaction was predominantly attributable to the linear component of bins [$F(1,38)=5.10$ $p<0.05$], which accounted for 80% of the variance explained by the three-way interaction. We therefore calculated the linear component for each group for additional post-hoc comparisons. A downward sloping trend was detectable in all groups, and their mean (±SEM) magnitudes are as follows, adult control = 0.63±0.98, adult mutant = 4.17±0.89, aged control = 0.99±0.82, aged mutant-=0.38± 0.98. The significantly higher value for the adult mutant [maximum $p=0.01$] than the other three groups (Figure 3C and 3F or 3I and 3L), which did not differ from each other, suggested that the linear rate of extinction within-session was the highest in the adult mutants.

Spontaneous recovery of conditioned CS freezing was evaluated by a 2 × 2 × 2 × 4 (genotype × age × days × 2-min bins) ANOVA that allowed a direct comparison of the animals' freezing response exhibited on the CS tests conducted before and after the 7-day retention period. As shown in Figure 4A, the CR recovered to a somewhat higher level, and mutant mice regardless of age, again, exhibited a stronger response than controls. The analysis yielded a significant effect of days suggestive of a spontaneous recovery effect [$F(1,38)=8.36$, $p<0.01$] as well as a significant genotype effect [$F(1, 38)=8.02$, $p<0.01$] (Figure 4B). Although aged mutant mice once again appeared to exhibit a weaker within-session extinction profile on this test, there was no evidence for a significant genotype by bins interaction [$F<1$], which might be due to the lack of a strong overall within-session extinction effect in this test, as suggested by the lack of a statistically significant bins effect [$F(3,114)=1.63$, $p>0.05$].

Immunohistochemistry

Visualization of apoptosis by Caspase-3 immunohistochemistry—The possible effect of forebrain neuronal GlyT1 knockout on apoptotic cell death was assessed by caspase-3 immunostaining. Caspase-3 is a cysteine protease and a key degradative enzyme involved in apoptosis (Rami, Jansen, Giesser, & Winckler, 2003). Quantification of caspase-3-ir cells did not reveal any difference between groups. The mean numbers of cells per unit volume (±SEM) were: control: adult=7.67 ± 2.7, aged=7.55 ± 2.36; mutant: adult=4.42 ± 2.46, aged=8.95 ± 3.09. A 2 × 2 (age × genotype) ANOVA of the number of the caspase-3-ir cells in the granular cell layer of the DG in the dHPC revealed neither a significant main effect of genotype and age nor its interaction.

NR1 and NR2B immunohistochemistry—None of the measurements revealed any genotype effect (see Table 2). Separate 2 × 2 (age × genotype) ANOVAs (per marker per region) only yielded a main effect of age in the analysis of CA3 NR2B immunodensity

[F(1,35)=7.74, p<0.05]. Representative photographs taken from each group are illustrated in Figure 5.

Visualization of immature neurons by doublecortin immunohistochemistry— Evaluation of the stereological estimates by a non-parametric ANOVA revealed a clear reduction in the number of DCX-positive cells in the aged animals as expected [F(1,34)=107.07; p<0.05] in comparison with the adults (Figure 6). Importantly, a significant genotype effect was also detected [F(1,34)=4.47; p<0.05] suggesting an increase in DCX-positive cells in the mutant mice. This effect did not appear to be significantly affected in senescence [Genotype × Age interaction: F(1,34)=0.36, p=0.55] in spite of the substantial age-related decrease.

Discussion

The present study replicated the robust effect of enhanced CS-freezing in young adult mice by GlyT1 deletion in forebrain neurons, and confirmed that this phenotype could also be detected in senescent age. As previously shown, this phenotype cannot be attributed to confounding changes in general anxiety or locomotor activity at either age (Yee *et al.*, 2006). However, examination of the temporal expression of the conditioned freezing response revealed clear differences between adult and aged mutants, while the freezing response was hardly modified by age in the control mice (Figures 3D and 3E). Thus, senescence had modified the behavioral effects of forebrain neuronal GlyT1 deletion. Parallel immunohistological examinations did not reveal any obvious changes in apoptosis in the hippocampus or NR1 and NR2 expression in multiple limbic cortices in the mutant mice. Surprisingly, we observed a pronounced enhancement of neural proliferation in the mutants which seemed to persist into senescence despite the drastic reduction due to aging.

The impact of aging in the mutants

Across the first two CS-test sessions, the temporal profile of CS-freezing in adult mutants is marked by (i) pronounced elevation of freezing close to CS-onset, and (ii) rapid within-session extinction across the continuous 8-min presentation of the CS, with freezing levels returning to adult controls' levels by session's end (see Figure 3G). The former was most clearly seen on the first CS-test day, whereas the latter persisted into the second and third test sessions albeit with a weaker impression (see Figures 3G & 4A). In comparison with adult mutants, the initial response near CS-onset was weaker in aged mutant mice, which also lacked the within-session extinction phenotype seen in the adult mutants, such that aged mutants exhibited stronger freezing than the other groups by session's end on the first two CS-test sessions (see Figure 3J). However, the lack of within-session extinction in the aged mutants might not be considered as a phenotype since within-session extinction was weak in control mice at both ages (see Figure 3D). The latter might be attributed to the reduced number of CS-US pairings adopted in this experiment, but it did not undermine the comparison between adult and aged mutants (Figures 3A, 3B and 3C), which indicated the loss of an important aspect of the adult CS-freezing phenotype, suggesting a (qualitative) diminution of the adult phenotype.

While there was statistical evidence for a within-session extinction phenotype that was affected by age, between-day extinction did not seem to be affected by GlyT1 deletion or age. Long-term extinction learning is believed to involve new learning, which acts to inhibit expression of the conditioned response (CR; Wagner, 1981; Wagner & Brandon, 2001). Dissipation of such inhibition in time revealed the spontaneous recovery effect (Rescorla, 2004) and confirmed that extinction did not lead to the erasure of the original CS-US memory trace. Intact retention of extinction learning from the first to the second CS-tests sessions (separated by 24h), and the re-emergence of the CR seven days later, suggest that

the mechanism underlying the control of new learning that underlies long-term extinction was relatively unaffected by GlyT1 deletion. What might be unique to within-session extinction in our paradigm?

Within-session extinction

Apart from new learning that directly competes or impedes CR during extinction, an independent process has been proposed by Wagner and Brandon (2001). This could be especially relevant to our test paradigm here, whereby the CS was presented continuously for a protracted period (Haselgrove & Pearce, 2003). According to Wagner & Brandon's model, prolonged exposure of a CS is expected to reduce its efficacy to evoke a CR, because perception of a stimulus steady in time and intensity is expected to first intensify (*temporal integration*) and then decline (*adaptation*). The model attributes this to a progressive shift of the stimulus representation from a primary active (A1) state to a secondary refractory (A2) state. When the CS representation is at the A2 state, its ability to activate the US representation is weakened and so is the evocation of the associated CR. However, when the CS representation departs from the A2 state and returns to its inactive baseline state, it can be readily re-activated to the A1 state when the stimulus reappears, thus again capable of recalling the US and therefore expression of the CR. This process therefore does not contribute significantly to the cessation of CR between-days. Thus, when the CS was presented in a test session the transition of the CS representation from A1 to A2 states might be facilitated in our adult mutant mice, but this facilitation might be selectively lost when they reached senescence.

This theoretical discourse would lead to the interesting prediction that associative learning might be weaker rather than stronger in the adult mutants (compared with adult controls) when the CS is extended in time during acquisition. It would predict that their CR would be weaker than controls when conditioned with an extended CS, but stronger with shorter CS. Thus far, we have obtained evidence that when CS and US are separated in time (i.e., trace conditioning) our mutant mice exhibited weaker freezing than control mice, which might be supportive of this interpretation (Singer et al., unpublished data). The apparent enhanced sensitivity to CS-US temporal discontinuity might again stem from a facilitated transition of the CS representation from A1 to A2 state.

The account based on Wagner's model shares some similarity with the attentional theory by Mackintosh (1974, 1975), which predicts that attention to a CS depends on its predictiveness of significant events (US's). Thus, attention to the CS would grow during acquisition but should decay during extinction. The decline in CR during extinction may then be attributed also to *in*attention to the CS. Indeed, such *in*attention to the CS is critical to the expression of latent inhibition (Lubow & Moore, 1959), which is facilitated also by forebrain neuronal GlyT1 deletion (Yee *et al.*, 2006). The present results might predict that the latent inhibition phenotype may be similarly attenuated as a function of age. This certainly warrants verification as it might bear implication on the proposed use of GlyT1 inhibitors as antipsychotic drugs (Javitt, 2009).

Effects in the brain

Consistent with our previous western blot analysis (Yee *et al.*, 2006), NR1 expression in the hippocampus of our mutant mice remained unaltered. We extended this null effect here to other brain structures, namely, the amygdala and prefrontal cortices. Likewise, NR2 expression was unaffected, including hippocampal NR2 expression which was particularly sensitive to aging (Magnusson, Nelson, & Young, 2002). These null findings collectively not only speak against compensatory changes in the NMDAR system and increases in NMDAR internalization resulting from excessive priming by extracellular glycine, but also

agree with the lack of changes in apoptosis observed in the hippocampus. Hence, there is little evidence here in support of the concern that forebrain neuronal GlyT1 deletion might induce neurotoxicity and/or undermine the integrity of NMDAR transmission in senescent mice. Indeed, increased activation of neuronal hippocampal glycine receptors (Xu and Gong, 2010) by elevated glycine might exert neuroprotective effects. Further investigations within and beyond the glutamatergic neurotransmission system are warranted to ascertain if loss of forebrain neuronal GlyT1 might accelerate the aging process in the brain. Similarly, examinations of caspase-independent apoptotic pathways would also be instructive (Abraham & Shaham, 2004).

Without any significant impact on NR1 or NR2 expression, the novel finding of enhanced hippocampal neural proliferation was revealed in our mutant mice. This was an unexpected finding since enhanced neurogenesis is linked to NMDAR blockade, and NMDAR activation to decreased neurogenesis (Cameron, McEwen, & Gould, 1995). This novel finding revealed here using doublecortin immunohistochemistry might be suggestive of an increase in the rate of neurogenesis, cell differentiation or survival/integration of new neurons (Li, Mu, & Gage, 2009), and additional markers (e.g., BrdU) are required to distinguish between these possibilities. Nonetheless, we have since replicated this finding in behaviorally naïve mice (S. Dubroqua, O. Raineteau, J. Feldon & B.K. Yee, unpublished data), thus excluding the possibility that prior behavioral testing was responsible for this new finding.

Although outside the scope of the present study, one may question the possible functional relevance of the neurogenesis phenotype. It might be tempting to link this to the conditioned freezing phenotype reported here as well as other learning-related phenotypes identified in this mutant mouse line thus far (Singer *et al.*, 2007, 2009; Yee *et al.*, 2006). Such speculations however would be premature given that the cause-and-effect relationship between neurogenesis and learning remains uncertain (Leuner, Gould, & Shors, 2006). Instead, this transgenic mouse model might be useful in assessing the impact of enhanced neurogenesis on learning, by identifying those phenotypes that might be eliminated specifically by neurogenesis suppressing treatments (e.g. Deng, Saxe, Gallina, & Gage, 2009; Winocur, Wojtowicz, Sekeres, Snyder, & Wang, 2006).

Conclusions

The present study has dispelled some concerns over possible negative side effects of long-term GlyT1 down-regulation, but also identified clear modification of a robust behavioral phenotype previously documented in the adult mutants with forebrain neuronal GlyT1 deletion. These are especially relevant to the potential use of GlyT1 inhibiting drugs in the context of age-dependent cognitive decline. The general importance of assessing genetic effects over the course of life is also highlighted by the present study.

Acknowledgments

The present study was supported by the Swiss Federal Institute of Technology Zurich and the National Institutes of Health (MH083973). The authors also thank Peter Schmid for the maintenance of behavioral testing equipments and preparation of the image analysis software, and the animal husbandry staffs for their excellent services. We also indebted to Byron Bitanihirwe for his editorial assistance in manuscript preparation. Sylvain Dubroqua and Philipp Singer were supported by the Neural Plasticity & Repair, National Centre for Competence in Research (NCCR), the Swiss National Science Foundation.

References

Abraham MC, Shaham S. Death without caspases, caspases without death. Trends in Cell Biology 2004;14:184–193. [PubMed: 15066636]

Bizon JL, Gallagher M. Production of new cells in the rat dentate gyrus over the lifespan: relation to cognitive decline. European Journal of Neuroscience 2003;18:215–219. [PubMed: 12859354]

Black MD, Varty GB, Arad M, Barak S, De Levie A, Boulay D, Pichat P, Griebel G, Weiner I. Procognitive and antipsychotic efficacy of glycine transport 1 inhibitors (GlyT1) in acute and neurodevelopmental models of schizophrenia: latent inhibition studies in the rat. Psychopharmacology (Berl) 2009;202:385–396. [PubMed: 18709358]

Budihardjo I, Oliver H, Lutter M, Luo X, Wang X. Biochemical pathways of caspase activation during apoptosis. Annual Review of Cell and Developmental Biology 1999;15:269–290.

Cameron HA, McEwen BS, Gould E. Regulation of adult neurogenesis by excitatory input and NMDA receptor activation in the dentate gyrus. Journal of Neuroscience 1995;15:4687–4692. [PubMed: 7790933]

Conover WJ, Iman RL. Rank transformation as a bridge between parametric and nonparametric statistics. American Statistician 1981;35:124–133.

Deng W, Saxe MD, Gallina IS, Gage FH. Adult-born hippocampal dentate granule cells undergoing maturation modulate learning and memory in the brain. Journal of Neuroscience 2009;29:13532–13542. [PubMed: 19864566]

Depoortere R, Dargazanli G, Estenne-Bouhtou G, Coste A, Lanneau C, Desvignes C, Poncelet M, Heaulme M, Santucci V, Decobert M, Cudennec A, Voltz C, Boulay D, Terranova JP, Stemmelin J, Roger P, Marabout B, Sevrin M, Vige X, Biton B, Steinberg R, Francon D, Alonso R, Avenet P, Oury-Donat F, Perrault G, Griebel G, George P, Soubrie P, Scatton B. Neurochemical, electrophysiological and pharmacological profiles of the selective inhibitor of the glycine transporter-1 SSR504734, a potential new type of antipsychotic. Neuropsychopharmacology 2005;30:1963–1985. [PubMed: 15956994]

Fritschy JM, Weinmann O, Wenzel A, Benke D. Synapse-specific localization of NMDA and GABA(A) receptor subunits revealed by antigen-retrieval immunohistochemistry. Journal of Comparative Neurology 1998;390:194–210. [PubMed: 9453664]

Gundersen HJ, Bagger P, Bendtsen TF, Evans SM, Korbo L, Marcussen N, Moller A, Nielsen K, Nyengaard JR, Pakkenberg B, et al. The new stereological tools: disector, fractionator, nucleator and point sampled intercepts and their use in pathological research and diagnosis. Apmis: Acta Pathologica, Microbiologica et Immunologica Scandinavica 1988;96:857–881.

Haselgrove M, Pearce JM. Facilitation of extinction by an increase or a decrease in trial duration. Journal of Experimemtal Psychology: Animal Behavior Processes 2003;29:153–166.

Javitt DC. Glutamate as a therapeutic target in psychiatric disorders. Molecular Psychiatry 2004;9:984–997. 979. [PubMed: 15278097]

Javitt DC. Glycine transport inhibitors for the treatment of schizophrenia: symptom and disease modification. Current Opinion in Drug Discovery & Development 2009;12:468–478.

Leuner B, Gould E, Shors TJ. Is there a link between adult neurogenesis and learning? Hippocampus 2006;16:216–224. [PubMed: 16421862]

Li Y, Mu Y, Gage FH. Development of neural circuits in the adult hippocampus. Current Topics in Developmental Biology 2009;87:149–174. [PubMed: 19427519]

Lubow RE, Moore AU. Latent inhibition: the effect of nonreinforced pre-exposure to the conditional stimulus. Journal of Comparative & Physiological Psychology 1959;52:415–419. [PubMed: 14418647]

Magnusson KR, Nelson SE, Young AB. Age-related changes in the protein expression of subunits of the NMDA receptor. Brain Research Molecular Brain Research 2002;99:40–45. [PubMed: 11869807]

Mackintosh, NJ. The psychology of animal learning. Academic press inc; London: 1974.

Mackintosh NJ. A theory of attention: Variations in the associability of stimuli with reinforcement. Psychological Review 1975;82:276–298.

Maren S. Neurobiology of Pavlovian fear conditioning. Annual Review of Neuroscience 2001;24:897–931.

Martin SJ, Grimwood PD, Morris RG. Synaptic plasticity and memory: an evaluation of the hypothesis. Annual Review of Neuroscience 2000;23:649–711.

Meyer U, Feldon J, Schedlowski M, Yee BK. Towards an immuno-precipitated neurodevelopmental animal model of schizophrenia. Neuroscience & Biobehavioral Reviews 2005;29:913–947. [PubMed: 15964075]

Morris RG. Synaptic plasticity and learning: selective impairment of learning rats and blockade of long-term potentiation in vivo by the N-methyl-D-aspartate receptor antagonist AP5. Journal of Neuroscience 1989;9:3040–3057. [PubMed: 2552039]

Morris RG, Anderson E, Lynch GS, Baudry M. Selective impairment of learning and blockade of long-term potentiation by an N-methyl-D-aspartate receptor antagonist, AP5. Nature 1986;319:774–776. [PubMed: 2869411]

Nong Y, Huang YQ, Ju W, Kalia LV, Ahmadian G, Wang YT, Salter MW. Glycine binding primes NMDA receptor internalization. Nature 2003;422:302–307. [PubMed: 12646920]

Rami A, Jansen S, Giesser I, Winckler J. Post-ischemic activation of caspase-3 in the rat hippocampus: evidence of an axonal and dendritic localisation. Neurochemistry International 2003;43:211–223. [PubMed: 12689601]

Rescorla RA. Spontaneous recovery. Learning & Memory 2004;11:501–509. [PubMed: 15466300]

Richmond MA, Murphy CA, Pouzet B, Schmid P, Rawlins JN, Feldon J. A computer controlled analysis of freezing behaviour. Journal of Neuroscience Methods 1998;86:91–99. [PubMed: 9894789]

Rosenzweig ES, Barnes CA. Impact of aging on hippocampal function: plasticity, network dynamics, and cognition. Progress in Neurobiology 2003;69:143–179. [PubMed: 12758108]

Rothman SM, Olney JW. Excitotoxicity and the NMDA receptor--still lethal after eight years. Trends in Neuroscience 1995;18:57–58.

Sanderson DJ, Bannerman DM. Supersmart mice: surprising or surprised? Theoretical comment on Singer, Boison, Mohler, Feldon, and Yee (2007). Behavioral Neuroscience 2007;121:1137–1139. [PubMed: 17907847]

Singer P, Boison D, Mohler H, Feldon J, Yee BK. Enhanced recognition memory following glycine transporter 1 deletion in forebrain neurons. Behavioral Neuroscience 2007;121:815–825. [PubMed: 17907814]

Singer P, Boison D, Mohler H, Feldon J, Yee BK. Deletion of glycine transporter 1 (GlyT1) in forebrain neurons facilitates reversal learning: enhanced cognitive adaptability? Behavioral Neuroscience 2009;123:1012–1027. [PubMed: 19824767]

Tsai G, Ralph-Williams RJ, Martina M, Bergeron R, Berger-Sweeney J, Dunham KS, Jiang Z, Caine SB, Coyle JT. Gene knockout of glycine transporter 1: characterization of the behavioral phenotype. Proceedings of the National Academy of Sciences U S A 2004;101:8485–8490.

Wagner, AR. SOP: A model of automatic memory processing in animal behavior. In: Spear, NE.; Miller, RR., editors. Information processing in animals: Memory mechanisms. Hillsdale, NJ: Erlbaum; 1981. p. 5-47.

Wagner, AR.; Brandon, SE. A componential theory of Pavlovian conditioning. In: Mowrer, RR.; Klein, SB., editors. Handbook of contemporary learning theories. Mahwah, NJ: Erlbaum; 2001. p. 23-64.

Walton JP, Barsz K, Wilson WW. Sensorineural hearing loss and neural correlates of temporal acuity in the inferior colliculus of the C57BL/6 mouse. Journal of the Association for Research in Otolaryngology 2008;9:90–101. [PubMed: 17994264]

Winocur G, Wojtowicz JM, Sekeres M, Snyder JS, Wang S. Inhibition of neurogenesis interferes with hippocampus-dependent memory function. Hippocampus 2006;16:296–304. [PubMed: 16411241]

Yang CR, Svensson KA. Allosteric modulation of NMDA receptor via elevation of brain glycine and D-serine: the therapeutic potentials for schizophrenia. Pharmacology & Therapeutics 2008;120:317–332. [PubMed: 18805436]

Yee BK, Balic E, Singer P, Schwerdel C, Grampp T, Gabernet L, Knuesel I, Benke D, Feldon J, Mohler H, Boison D. Disruption of glycine transporter 1 restricted to forebrain neurons is associated with a procognitive and antipsychotic phenotypic profile. Journal of Neuroscience 2006;26:3169–3181. [PubMed: 16554468]

Yee BK, Hauser J, Dolgov VV, Keist R, Mohler H, Rudolph U, Feldon J. GABA receptors containing the alpha5 subunit mediate the trace effect in aversive and appetitive conditioning and extinction of conditioned fear. European Journal of Neuroscience 2004;20:1928–1936. [PubMed: 15380015]

Yee BK, Singer P, Chen JF, Feldon J, Boison D. Transgenic overexpression of adenosine kinase in brain leads to multiple learning impairments and altered sensitivity to psychomimetic drugs. European Journal of Neuroscience 2007;26:3237–3252. [PubMed: 18005073]

Xu TL, Gong N. Glycine and glycine receptor signaling in hippocampal neurons: diversity, function and regulation. Progress in Neurobiology 2010;91:349–361. [PubMed: 20438799]

Figure 1.
Spontaneous locomotor activity in the open field (OF) shown as total distance travelled per 10 min bins. All values refer to mean±SEM.

Figure 2.
The acquisition of conditioned freezing to the tactile CS on day 1 (A) and context freezing on day 2 (B) are depicted. All values refer to mean±SEM.

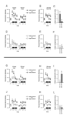

Figure 3.

Freezing to the vibration CS in the first and second CS test sessions (conducted 48 h and 72 h after conditioning, respectively) is depicted in two perspectives: (a) comparison of age of each phenotype, and (b) comparison of genotypes at each age. They are demarcated by the horizontal line in the middle. ***A***, ***D***, ***G***, and ***J*** depict the percent time freezing across successive 2-min bins (including the pre-CS bin denoted as "P*" in the x-axis) on the two separate CS tests. ***B***, ***E***, ***H***, and ***K*** represent the same data when collapsed across the two test sessions. Following the emergence of the significant Genotype × Age × Bins interaction which was predominantly attributable to the linear trend, the linear components of the Bins effect (collapsed across test sessions) in each group was calculated and depicted in ***C***, ***F***,***I***, and ***L***. Post-hoc comparisons based on the appropriate error mean square terms taken from the overall ANOVA were performed at successive bins and significant pair-wise differences are denoted by asterisks in the appropriate graphs. All values refer to mean±SEM.

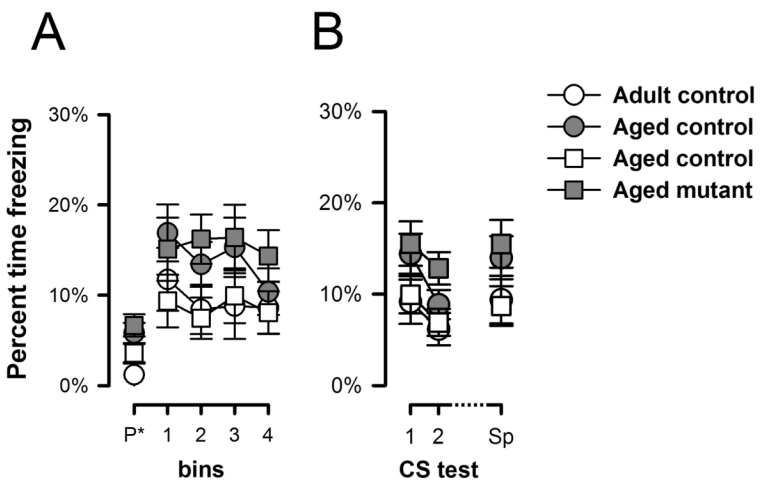

Figure 4.

Freezing to the CS 7 days after the last CS-test (A) and overall freezing for the 3 CS-test (B) are depicted. Percent time freezing is indexed as a function of 2-min bins including the 2 minutes of pre-CS. Sp refer to the CS 7 days after the last CS-test. All values refer to mean ±SEM.

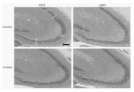

Figure 5.
Representative photomicrographs of NR2B immunostaining in the dHPC. (scale bar = 100 μm)

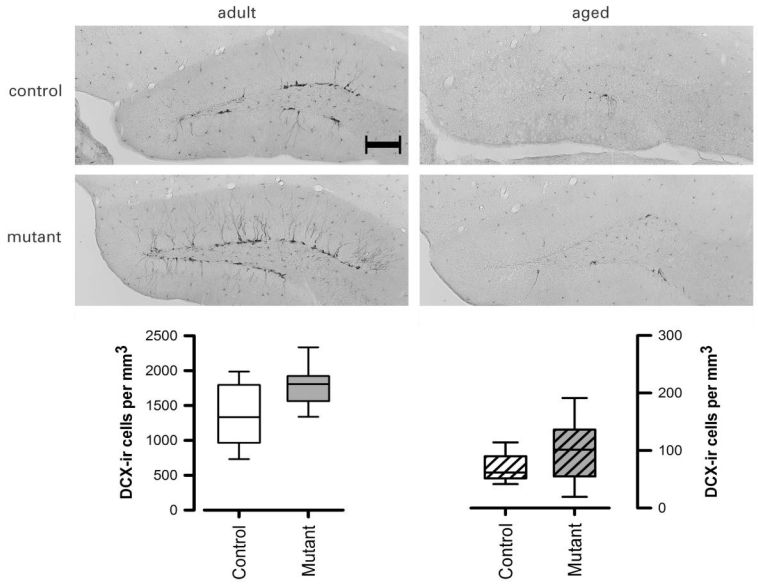

Figure 6.

Representative photomicrographs of doublecortin-positive (DCX) immunostaining (scale bar = 200 μm). Separate box-plots showing the stereological estimates of DCX-positive cells per unit volume in the dentate gyrus granule cell layers. Each box plot captures the data within the inter-quartile range in the box. The group median is represented by the horizontal line inside each box. The upper and lower whiskers represent the boundaries of the largest and lowest values within each group. All data refers to the original untransformed data set, and their depiction is appropriate for the non-parametric (Genotype × Age) ANOVA performed, which yielded a significant main effect of Genotype and of Age.

Table 1

Anxiety-like behavior in the elevated plus maze (EPM) as indexed by (i) percentage of entries made into the open arms, and (ii) percentage of time spent in the open arms. Spontaneous locomotor activity was indexed by total distance travelled in the elevated plus maze. All values refer to mean±SEM.

Measure	Control		Mutant	
	Adult	Aged	Adult	Aged
Anxiety in the EPM				
Percent open arms entries	31.1±3.4	35.2±4.6	38.05±5.2	37.8±5.5
Percent time in open arms	21.5±6.0	32.2±7.0	27.3±8.8	32.5±8.0
Percent distance in open arms	14.6±4.0	24.6±5.1	22.8±8.4	24.6±5.1
Locomotor activity in EPM				
Distance moved [m]	6.9±0.7	6.5±0.6	5.9±0.3	6.1±0.8

Table 2

Summary of the relative optical densities of NMDA receptor subunit 1 (NR1) and NMDA receptor subunit 2B (NR2B) in the subregions of the dHPC (CA1/2 and CA3), Amygdala (BLA and CeA) and Prefrontal cortex (Cg1, PrL and IL) of adult and aged mutant and control mice. Values refer to mean±SEM.

	Control		Mutant	
	Adult	**Aged**	**Adult**	**Aged**
NR1				
Hippocampus				
CA1/2	61.9±3.6	63.8±3.1	63.76±3.30	66.25±4.08
CA3	60.8±3.3	59.0±2.8	60.49±2.94	61.93±3.68
Amygdala				
BLA	29.62±2.11	25.39±1.83	27.41±2.0	27.68±2.39
CeA	33.20±2.29	29.38±1.98	30.74±2.17	32.23±2.60
PFC				
Cg1	22.84±2.34	17.34±2.02	21.67±2.22	20.55±2.65
PrL	30.11±2.22	26.92±1.92	31.26±2.10	26.70±2.51
IL	33.06±2.84	30.24±2.46	34.67±2.69	28.39±3.22
NR2B				
Hippocampus				
CA1/2	64.9±2.0	62.5±1.7	67.2±1.8	62.0±2.3
CA3	59.9±2.0	55.3±1.8	61.1±1.8	54.5±2.3
Amygdala				
BLA	44.0±2.9	45.0±2.5	50.4±2.8	46.0±3.3
CeA	56.2±2.7	55.5±2.4	57.5±2.6	55.4±3.1
PFC				
Cg1	32.8±2.4	29.7±2.1	33.9±2.3	34.1±2.7
PrL	37.0±2.4	37.5±2.0	40.9±2.2	39.2±2.7
IL	40.5±2.9	41.6±2.5	46.0±2.7	41.2±3.3